Proc. Natl. Acad. Sci. USA
Vol. 89, pp. 10124–10128, November 1992
Biophysics

Comparison of the NMR solution structure and the x-ray crystal structure of rat metallothionein-2

W. BRAUN*, M. VAŠÁK†, A. H. ROBBINS‡, C. D. STOUT§, G. WAGNER¶, J. H. R. KÄGI†, AND K. WÜTHRICH*

*Institut für Molekularbiologie und Biophysik, Eidgenössische Technische Hochschule, Hönggerberg, CH-8093 Zürich, Switzerland; †Biochemisches Institut, Universität Zürich, CH-8057 Zürich, Switzerland; ‡Miles Research Center, West Haven, CT 06516; §Scripps Research Institute, La Jolla, CA 92037; and ¶Department of Biological Chemistry and Molecular Pharmacology, Harvard Medical School, Boston, MA 02115

Contributed by K. Wüthrich, July 13, 1992

ABSTRACT **Metallothioneins are small cysteine-rich proteins capable of binding heavy metal ions such as Zn^{2+} and Cd^{2+}. They are ubiquitous tissue components in higher organisms, which tentatively have been attributed both unspecific protective functions against toxic metal ions and highly specific roles in fundamental zinc-regulated cellular processes. In this paper a detailed comparison of the NMR solution structure [Schultze, P., Wörgötter, E., Braun, W., Wagner, G., Vašák, M., Kägi, J. H. R. & Wüthrich, K. (1988) *J. Mol. Biol.* 203, 251–268] and a recent x-ray crystal structure [Robbins, A. H., McRee, D. E., Williamson, M., Collett, S. A., Xoung, N. H., Furey, W. F., Wang, B. C. & Stout, C. D. (1991) *J. Mol. Biol.* 221, 1269–1293] of rat metallothionein-2 shows that the metallothionein structures in crystals and in solution have identical molecular architectures. The structures obtained with both techniques now present a reliable basis for discussions on structure–function correlations in this class of metalloproteins.**

Mammalian metallothioneins (MTs) are small proteins with 61 or 62 amino acid residues that have the ability to accommodate metal ions of different size and chemical reactivity without compromising the overall molecular architecture (1–4). This observation has been used to support the hypothesis that the primary function of MTs is to shield cellular structures from the harmful influence of toxic metals such as cadmium, mercury, platinum, bismuth, silver, and gold by limiting the intracellular concentration of these heavy metal ions (5, 6). In addition to such rather unspecific protective functions, recent findings imply that MTs have a more specific major role in fundamental zinc-related cellular processes, with thionein supplied by controlled biosynthesis regulating the flow of zinc(II) within the cell and thereby modulating the action of zinc-dependent processes in response to signals for cell activation in proliferation and differentiation (4, 7–9). An assessment of these suggested MT functions on the molecular level has so far been limited by the fact that a MT structure determined by x-ray diffraction in single crystals (10) had a different molecular architecture from that in MT structures determined by NMR spectroscopy in solution (2, 11, 12). Subsequently it was found that the crystal structure needed to be revised, and a new crystal structure of rat MT2 was presented (3) that has the same overall architecture as the NMR structure (2). To provide a reliable basis for investigations on structure–function correlations in MTs, this paper now describes a detailed comparison of the structures of rat MT2 in crystals and in solution.‖

METHODS

The NMR solution structure of rat heptacadmium(II) metallothionein II ([Cd_7]-MT2) (2) was characterized in the usual way (13) by a group of 10 conformers obtained from the NMR data with distance geometry calculations (14–16). The structure consists of two domains containing, respectively, residues 1–30 and three Cd^{2+} ions (β domain) and residues 31–61 and four Cd^{2+} ions (α domain). The two domains are connected by a flexible polypeptide segment, and their relative positions have not been determined. Therefore, all structure comparisons have been performed separately for the α and β domains. The quality of the structure determination as indicated by the closeness of coincidence of the 10 conformers is defined by the root-mean-square deviations (rmsd) between the individual NMR conformers and the mean solution structure (Table 1). The new x-ray crystal structure of [Cd_5, Zn_2]-MT2 (containing four Cd^{2+} ions in the α domain and two Zn^{2+} ions and one Cd^{2+} ion in the β domain) (3) was determined at a resolution of 2.0 Å and refined to a R value of 0.176. The crystal packing includes (*i*) intimately associated pairs of MT molecules related by a twofold symmetry axis and (*ii*) trapped ions of crystallization. The latter have been modeled as phosphate and sodium.

RESULTS AND DISCUSSION

Fig. 1 shows that for the two domains of rat MT2, the global polypeptide fold is closely similar in the crystal structure (3) and in solution (2). In the β domain the polypeptide chain wraps around the cysteine–metal cluster in a right-handed way, and in the α domain, in a left-handed way. The largest deviations between crystal and solution structure occur in the β domain—i.e., in the loop region from Thr-9 to Ser-12 and the C-terminal segment from Cys-24 to Lys-30, where the NMR conformer is clearly outside the circles representing the crystallographic B-factors (Fig. 1). These differences could be caused by crystal packing effects, as has also been observed elsewhere—for example, between corresponding surface residues in the solution and crystal structures of plastocyanin (17). In rat MT2 crystals the molecules are packed as interdigitated dimers about twofold axes (3). Residues of the β domain which have main-chain atoms involved in crystal-packing contacts include Thr-9, Ser-14, Cys-15, Cys-21, Lys-22, Cys-24, and Lys-30 (18), which also show the largest displacements between the two structures (Fig. 1*A*). However, the β domain is also generally less well defined by the NMR data than the α domain (Table 1), allowing for the possibility that the apparent deviations reflect increased dynamic disorder in the solution structure. In the α-domain the only apparent significant structural differences are seen for the N-terminal dipeptide (which

The publication costs of this article were defrayed in part by page charge payment. This article must therefore be hereby marked "*advertisement*" in accordance with 18 U.S.C. §1734 solely to indicate this fact.

Abbreviations: MT, metallothionein; rmsd, root-mean-square deviation(s).

‖The atomic coordinates of the NMR solution structure and the x-ray crystal structure have been deposited with the Brookhaven protein data bank with the following codes: 1MRT, α domain of rat MT2, NMR; 2MRT, β domain of rat MT2, NMR; 3MT2, x-ray crystal structure of rat MT2.

Table 1. rmsd values calculated for different selections of atoms between the x-ray crystal structure and the NMR solution structure of rat MT2

Domain	Atoms considered*	rmsd, Å	
		NMR:x-ray†	NMR:NMR‡
β	bb 1-30	2.4 (0.3)	2.0 (0.3)
	bb(3-9,12-29)	2.0 (0.3)	1.6 (0.3)
	bb 1-30 + Cys + Cd^{2+}/Zn^{2+}	2.2 (0.3)	1.8 (0.3)
	bb(3-9,12-29) + Cys + Cd^{2+}/Zn^{2+}	1.8 (0.2)	1.5 (0.3)
	S^{γ} + Cd^{2+}/Zn^{2+}	0.6 (0.2)	0.5 (0.2)
α	bb 31-61	1.9 (0.1)	1.7 (0.2)
	bb 31-61 + Cys + Cd^{2+}	1.7 (0.1)	1.6 (0.2)
	S^{γ} + Cd^{2+}	0.8 (0.2)	0.8 (0.2)

*bb, backbone atoms N, C^{α}, and C′ of the residues specified by the sequence positions; Cys, all heavy atoms of the cysteine side chains; Cd^{2+} and Zn^{2+}, metal ions in the two domains; and S^{γ}, sulfur atoms of all 20 cysteine residues.

†Average of the rmsd values for the pairwise comparisons of the x-ray crystal structure to the 10 NMR conformers representing the solution structure. The numbers in parentheses are the standard deviations.

‡Average of the rmsd values for the comparisons between all pairwise combinations of the 10 NMR conformers. The values in parentheses are the standard deviations. These data were adapted from ref. 2.

corresponds to the linker peptide between the two domains in the intact MT2 molecule) and for the segment Ala-53 to Asp-55. The latter forms part of the loop of residues 51–56, which is poorly defined in the crystal structure, with all temperature factors larger than 40 Å (3). These visual impressions are confirmed by the rmsd values between crystal and solution structures (Table 1). For the α domain the differences between the NMR conformers and the x-ray

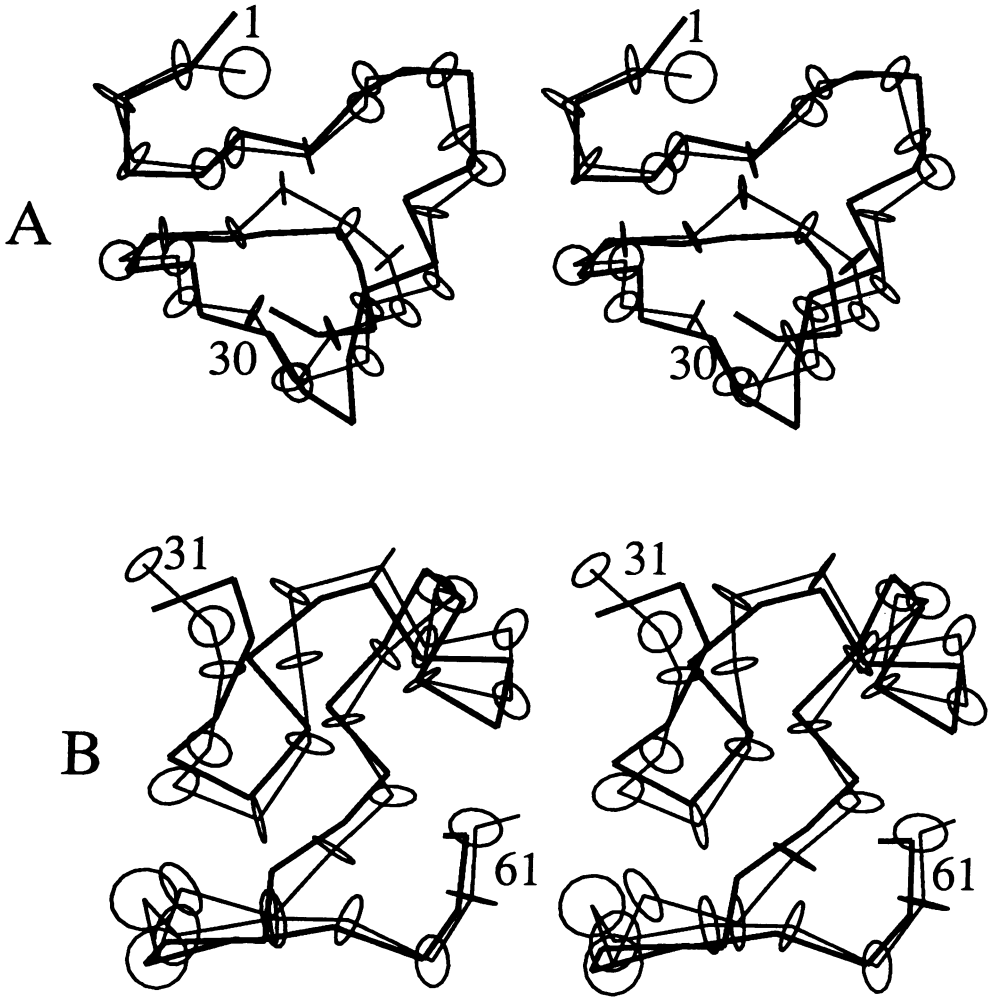

FIG. 1. Stereo views of best-fit superpositions of the polypeptide backbone in the x-ray crystal structure of rat $[Cd_5,Zn_2]$-MT2 (thin lines) (3) with the NMR conformer of $[Cd_7]$-MT2 that had the smallest residual error function value (thick line) (2). The backbone is represented by virtual bonds linking the α-carbon positions. For the x-ray structure the circles centered at the C^{α} positions represent the thermal factors, B, of the C^{α} atoms, with the radius calculated as $r = (3B/8\pi^2)^{1/2}$. (*A*) β domain with residues 1–30. (*B*) α domain with residues 31–61.

structure are virtually identical to the deviations within the ensemble of the NMR conformers, and for the β domain they are only slightly larger. It is interesting that the rmsd values calculated with inclusion of all cysteinyl side chains and the metal ions are smaller than those for the backbone atoms alone, indicating that the relatively large values for the polypeptide backbone are primarily a consequence of the intrinsically more flexible polypeptide backbone in MTs as compared with other proteins with a higher content of regular secondary structure. This conclusion receives further support from the fact that for all three MTs studied in solution (2, 11, 12) relatively large rmsd values were obtained for the groups of NMR conformers used to represent the solution structure (3).

To relate local differences between crystal and solution structure with the uncertainties in the two structure determinations, the B-factors of the x-ray structure on the level of the individual amino acid residues were compared to the corresponding rmsd values within the group of NMR conformers used to represent the solution structure (Table 1). For the x-ray structure, we first calculated the average of the B-factors for the backbone atoms N, C^{α}, and C′ for each residue, and then rmsd were calculated as rmsd = $(3B/8\pi^2)^{1/2}$. For the NMR structure, each of the other nine conformers was first fitted to the best conformer [i.e., the conformer with the smallest residual target function value (2)]. Then the average of the distance deviations for each of the backbone atoms was calculated over all nine pairs (rmsd values). In Fig. 2, the average of the rmsd values for the three backbone atoms N, C^{α}, and C′ of each residue was plotted versus the amino acid sequence. Crosses indicate the rmsd of the backbone atoms among the 10 NMR conformers, and circles show rmsd values for the x-ray structure. The outstandingly large deviations at residues 30–32, which is the linker region between the two domains, are not significant

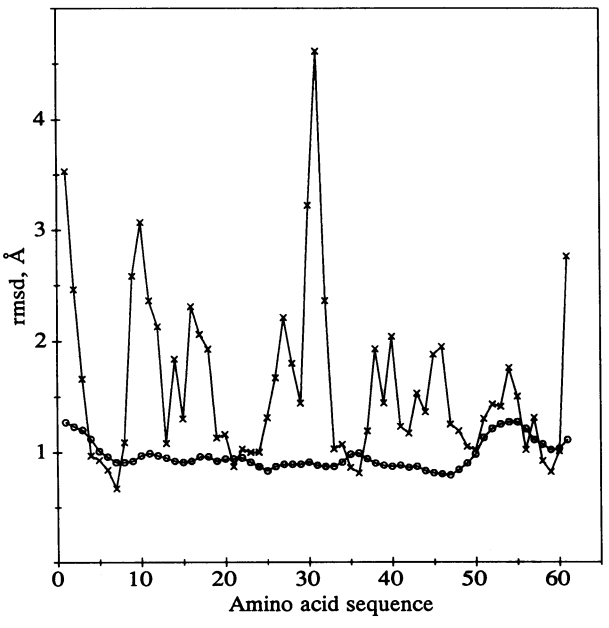

FIG. 2. Comparison of the spread of the 10 rat MT2 NMR conformers as indicated by the rmsd values (×) and the B-factors of the x-ray crystal structure (○). The B-factors are plotted as rmsd obtained as described in the text. For the NMR structures, each of the other nine conformers was globally superimposed to the best conformer, and then the average of the rmsd for each of the backbone atoms was calculated as described in the text. As the two domains have been separately determined by the NMR method, the global best fit was done separately for the α and the β domains. The crosses represent the average rmsd values over the three backbone atoms N, C^{α}, and C′ for each residue.

because the crystal structure determination was performed for the intact polypeptide chain, whereas the two domains were treated separately in the NMR structure determination (2), so that artifactual chain-termination effects resulted for these residues. The figure shows that for most of the polypeptide chain, the rmsd values of the x-ray structure present a lower limit for the rmsd values of the NMR structure. There is no obvious correlation between the variations of the rmsd values along the sequence derived from the two methods, which contrasts with observations made, for example, in the case of the α-amylase inhibitor Tendamistat (19). This might be due to the fact that there are no regular secondary structures and no hydrophobic core in MT2.

To complement the global comparisons for the polypeptide backbone on the level of individual amino acid residues, the dihedral angles ϕ and ψ were calculated from the atomic coordinates deposited in the Brookhaven protein data bank.‖ For the ten NMR conformers the mean values and the rmsd of the individual backbone dihedral angles were evaluated. It was then found that for nearly all residues, the differences between the dihedral angles of the x-ray structure and the mean of the dihedral angles among the NMR conformers are less than this rmsd value. Larger deviations prevail for the segments Cys-Ala-Gly at positions 15–17 and Lys-Glu-Ala-Ser-Asp at positions 51–55. The latter segment was previously mentioned as being poorly defined by the x-ray data, and there is the implication that the observed apparent differences in this region reflect structural disorder rather than a significant difference between crystal and solution. In the segment from position 15 through 17, Ala-16 has a positive ϕ angle in both structures, indicating that the conformation is sterically strained. An additional comment must be made about the local conformation in Cys-Xaa-Cys segments. In the x-ray crystal structure of rat MT2, all seven such segments were found to have similar conformations for the first two residues, with average values of the ϕ and ψ angles of −97° and 145° for the first cysteine, and −98° and 1° for the residue Xaa. In the crystal structure description, this type of local conformation was suggested to mimic a type I reverse turn (3). In the NMR structure, four of the seven Cys-Xaa-Cys segments are well defined, with average ϕ and ψ values of −50° and 111° for the first cysteine and −105° and 21° for the residue Xaa (2). Similar local conformations in the two structures are thus defined by these dihedral angles, but there is a significant deviation from type I tight turns, in which the first residue would have a ψ angle of −30°. Therefore, it was previously suggested that these segments form an unusual type of secondary structure—i.e., a half-turn (20). The new crystal structure now provides additional support for the occurrence of these half-turns.

Fig. 3 shows a detailed comparison of the metal–cysteinyl clusters in rat MT2 in crystals and in solution. The metal–sulfur bonds and the local chiralities of the four sulfur atoms around each of the tetrahedrally coordinated metal ions are the same in both structures. The local chirality at two metal ions in each cluster is right-handed [i.e., the four coordinated sulfur atoms form a right-handed loop when arranged in the order of the cysteine residue sequence numbers (11)], and left-handed around the other metal ions. As indicated by the rmsd values in Table 1, the cluster geometry and the conformation of the attached side chains of the cysteinyl residues are nearly identical in the two structures. The cluster geometries can best be described as distorted boat forms. The close coincidence of the cysteinyl side-chain conformations in the crystal and in solution was confirmed by an analysis of the side-chain dihedral angles χ^1 and χ^2, which agreed within the precision of the structure determinations for all residues except Cys-19, which forms part of a phosphate binding site in the crystal lattice.

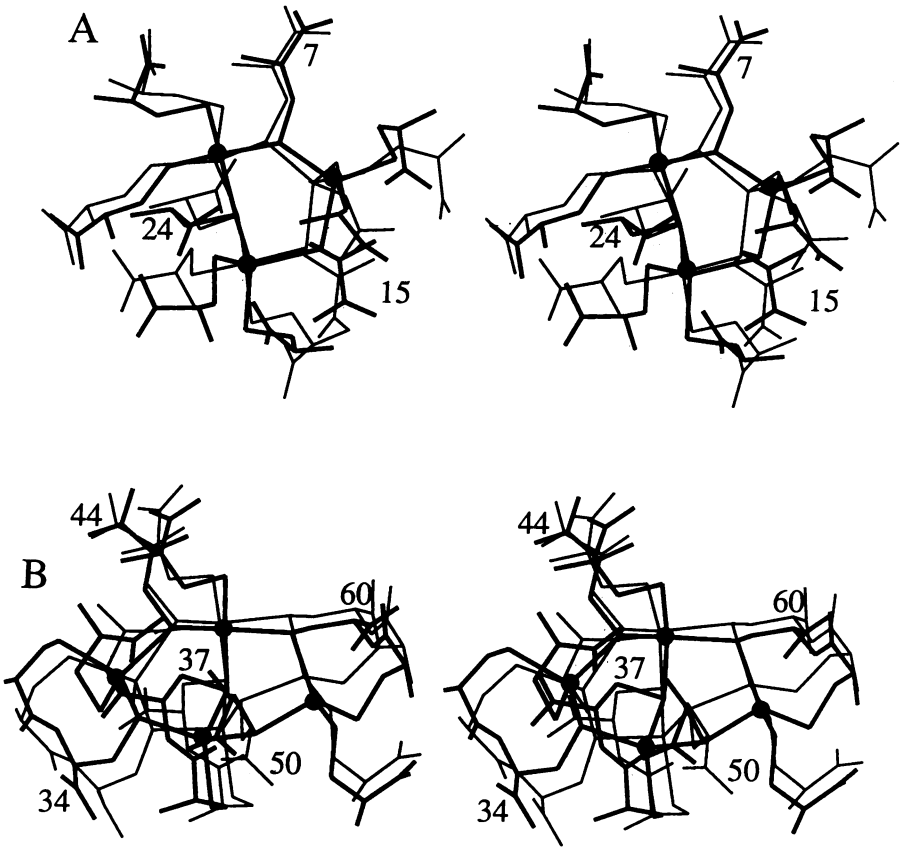

FIG. 3. Stereo views of best fit superpositions of the metal–cysteinyl clusters in rat MT2, with the x-ray crystal structure drawn with thin lines and the NMR solution structure with thick lines [the conformer with the smallest residual target function value (2) is again used to represent the NMR structure]. The bonds between all heavy atoms of the cysteine side chains as well as the sulfur–metal bonds are represented by straight lines, and the metal positions of the NMR structure are shown as black spheres. (*A*) β domain. Three metal ions are tetrahedrally coordinated by six singly bound cysteine residues and three bridging cysteine residues. The NMR structure contains three Cd^{2+} ions, and the x-ray structure contains two Zn^{2+} ions and one Cd^{2+} ion. (*B*) α domain. Four Cd^{2+} ions are tetrahedrally coordinated by 11 cysteine residues of which 5 are bridging cysteine residues bound to two metal ions. In both domains the bridging cysteine residues are labeled with their sequence numbers.

A detailed comparison of the noncysteinyl side chains seemed not warranted because most of these either are glycine, alanine, or serine, for which the conformation is largely characterized by the backbone dihedral angles ϕ and ψ, or are lysine, which is not well defined by the NMR data. Instead, the accessible surface areas in the x-ray crystal structure and in the 10 NMR conformers have been calculated with the program ANAREA (21). For nearly all residues, the accessible surface area of the x-ray structure was found to fall within the ranges defined by the ensemble of the NMR conformers, showing that the surface properties of MT2 in the two environments are in quite good agreement.

In conclusion, the key message from the present comparative studies is that in contrast to the data available during the period 1986–1990 (2, 10, 11), rat MT2 has the same molecular architecture in crystals and in solution. It is remarkable that even in the case of this flexible molecule, the NMR structure could be used as a starting model to interpret the initial electron density map, a procedure that has been successfully applied also with other proteins, for example tendamistat (22) and interleukin-8 (23). In both environments the protein consists of the same two domains, has identical polypeptide–metal coordinative bonds and metal–sulfur cluster geometries, and closely similar polypeptide folds. By either technique, but in particular in the solution structure, the polypeptide loops linking the metal-bound cysteine residues are less precisely defined than what is generally observed in proteins with a high content of regular secondary structure, indicating a considerable degree of dynamic structural disorder. This presents a possible explanation for the astonishing property of the metallothioneins to accommodate metals of widely differing size such as zinc ("covalent" atomic radius, 131 pm) and cadmium ("covalent" atomic radius, 148 pm) in the interior of the globular domains without causing gross conformational changes in the enfolding protein (1–4). This could provide a basis for both the presumed protection function of MTs against a wide spectrum of toxic metal ions (5, 6) and more specific regulatory functions, depending on subtle equilibria in the binding and release of Zn^{2+} ions by MT (4, 7–9).

This work was supported by the Schweizerische Nationalfonds (Projects 31.25174.88 and 3.160.88) and by National Institutes of Health Grant GM-36535. We thank Mr. R. Marani for the careful processing of the manuscript.

1. Vašák, M., Wörgötter, E., Wagner, G., Kägi, J. H. R. & Wüthrich, K. (1987) *J. Mol. Biol.* **196**, 711–719.
2. Schultze, P., Wörgötter, E., Braun, W., Wagner, G., Vašák, M., Kägi, J. H. R. & Wüthrich, K. (1988) *J. Mol. Biol.* **203**, 251–268.
3. Robbins, A. H., McRee, D. E., Williamson, M., Collett, S. A., Xoung, N. H., Furey, W. F., Wang, B. C. & Stout, C. D. (1991) *J. Mol. Biol.* **221**, 1269–1293.
4. Messerle, B., Schäffer, A., Vašák, M., Kägi, J. H. R. & Wüthrich, K. (1992) *J. Mol. Biol.* **225**, 433–443.
5. Nordberg, M. & Kojima, Y. (1979) *Experientia Suppl.* **34**, 41–117.
6. Webb, M. (1987) *Experientia Suppl.* **52**, 109–134.
7. Hamer, D. H. (1986) *Annu. Rev. Biochem.* **55**, 913–951.
8. Kägi, J. H. R. & Schäffer, A. (1988) *Biochemistry* **27**, 8509–8515.
9. Karin, M. (1985) *Cell* **41**, 9–10.

10. Furey, W. F., Robbins, A. H., Clancy, L. L., Winge, D. R., Wang, B. C. & Stout, C. D. (1986) *Science* **231**, 704–710.
11. Arseniev, A., Schultze, P., Wörgötter, E., Braun, W., Wagner, G., Vašák, M., Kägi, J. H. R. & Wüthrich, K. (1988) *J. Mol. Biol.* **201**, 637–657.
12. Messerle, B., Schäffer, A., Vašák, M., Kägi, J. H. R. & Wüthrich, K. (1990) *J. Mol. Biol.* **214**, 765–779.
13. Wüthrich, K. (1986) *NMR of Proteins and Nucleic Acids* (Wiley, New York).
14. Braun, W. (1987) *Q. Rev. Biophys.* **19**, 115–157.
15. Wüthrich, K. (1989) *Science* **243**, 45–50.
16. Braun, W. & Gō, N. (1985) *J. Mol. Biol.* **186**, 611–626.
17. Moore, J. M., Lepre, C. A., Gippert, G. P., Chazin, W. J., Case, D. A. & Wright, P. E. (1991) *J. Mol. Biol.* **221**, 533–555.
18. Robbins, A. H. & Stout, C. D. (1991) *Methods Enzymol.* **205**, 485–502.
19. Billeter, M., Kline, A. D., Braun, W., Huber, R. & Wüthrich, K. (1989) *J. Mol. Biol.* **206**, 677–687.
20. Wagner, G., Neuhaus, D., Wörgötter, E., Vašák, M., Kägi, J. H. R. & Wüthrich, K. (1988) *J. Mol. Biol.* **187**, 131–135.
21. Richmond, T. (1984) *J. Mol. Biol.* **178**, 63–89.
22. Braun, W., Epp, O., Wüthrich, K. & Huber, R. (1989) *J. Mol. Biol.* **206**, 669–676.
23. Baldwin, E. T., Weber, I. T., St. Charles, R., Xvan, J. C., Appella, E., Yamada, M., Matsushima, K., Edwards, B. F. P., Clore, G. M., Gronenborn, A. M. & Wlodawer, A. (1991) *Proc. Natl. Acad. Sci. USA* **88**, 502–506.